Renormalization group circuits for gapless states

Brian Swingle, John McGreevy, and Shenglong Xu

Renormalization Group Circuits for Gapless States

Brian Swingle,[1] John McGreevy,[2] and Shenglong Xu[2]

[1]*Department of Physics, Stanford University, Palo Alto, CA 94305, USA*
[2]*Department of Physics, University of California at San Diego, La Jolla, CA 92093, USA*

We show that a large class of gapless states are renormalization group fixed points in the sense that they can be grown scale by scale using local unitaries. This class of examples includes some theories with dynamical exponent different from one, but does not include conformal field theories. The key property of the states we consider is that the ground state wavefunction is related to the statistical weight of a local statistical model. We give several examples of our construction in the context of Ising magnetism.

I. INTRODUCTION

In this work we are interested in the entanglement structure of quantum critical points. These are systems where, in the thermodynamic limit, the spectrum of the Hamiltonian has no energy gap and the system displays scale invariant physics. Much effort has been expended to quantify entanglement in quantum critical points using entanglement entropy, but such a characterization is only the first step towards a complete understanding of the entanglement structure of these states of matter. A more refined characterization of the pattern of entanglement is provided by a quantum circuit which produces the state of interest from a product state—in essence we seek a set of instructions for building up the entanglement in the state from elementary ingredients.

Based on the scale invariance of the physics we expect the entanglement to be organized in a scale invariant way. This expectation is encoded in various circuit networks which have been conjectured to be capable of well approximating the ground state wavefunction of scale invariant states. These networks include multiscale entanglement renormalization ansatz (MERA)[1] and branching MERA[2] and the more general notion of s source renormalization group circuits or "s sourcery"[3]. However, while it is physically quite reasonable to conjecture that such circuits can well approximate the ground state, the actual evidence that this is true is scarce. In one dimension there is excellent numerical evidence that MERA well approximates the states of simple conformal field theories[4]. In higher dimensions the primary evidence comes from free field theory[5–7] and from holographic models[8]; in the latter case it was proposed that the geometry of the quantum circuit was related to the emergent holographic geometry. Moreover, we have very little information about the degree of approximation involved in using such a scale invariant circuit with a fixed bond dimension (the range of the indices of the tensors constituting the circuit).

The purpose of this paper is to partially remedy the above deficiencies by producing renormalization group circuits for certain wavefunctions supporting scale invariant physics. We are motivated by a desire to make progress – rigorous if possible – showing that gapless quantum phases and quantum critical points can be accurately captured, at the level of wavefunctions, within a renormalization group (RG) framework, along the lines of[3]. Specifically, we will show that a large class of such states are $s = 1$ RG fixed points in the sense defined in[3]: the state of the system at linear size L related to the state of the system at linear size $2L$ by a local isometry (or a unitary when ancilla degrees of freedom are included). More broadly the goals are: (1) to further our understanding of the entanglement structure of quantum matter, *e.g.* for simulation purposes, and (2) to better understand the holographic emergence of gravity from entanglement (in certain quantum field theories) using the tool of tensor networks[8–12].

Viewed as variational ansatz, the s sourcery framework is only slightly more expressive than MERA and branching MERA: s sourcery relaxes the requirement of strict circuit locality that is present in MERA. Indeed, both networks can be variationally determined by minimizing the energy with respect to a specified Hamiltonian. However, the s sourcery framework embodies a more general idea: it should be possible to determine renormalization group transformations locally in scale, i.e. without performing a global optimization. A comparison to Wilsonian momentum shell RG is instructive: integrating out high momentum modes does not require any knowledge of the fate of the theory in the IR (one could say that this is almost the whole point of Wilsonian RG). It may be difficult to carry out the RG due to strong coupling, but in principle we do not need to know what it happening in the IR until we get there. RG circuits for topological states of matter were constructed non-variationally in[3]. Here we do the same for a particular class of scale invariant gapless states of matter. We rely only on local-in-scale data to construct the RG circuit, thus explicitly realizing one of the key elements of the s sourcery program. We also note that the RG circuits we obtain, when viewed as local quantum circuits, have a range that depends weakly (logarithmically) on system size, but these circuits fit naturally into the s sourcery framework which allows this mild extra freedom.

The class of wavefunctions we are interested in are those that arise from the statistical weight of a classical statistical model[40]. Let us work with spins Z_r (r labels sites of a lattice) for concreteness (generalizations are obviously possible). Given a classical Hamiltonian $h(Z)$ we form the quantum wavefunction

$$\psi(Z; h, \beta) = \sqrt{\frac{e^{-\beta h(Z)}}{\mathcal{Z}}} \tag{1.1}$$

where β is a temperature we choose and $\mathcal{Z}$ is the classical partition function of the statistical model determined by h and β.[41] We call such a state a square root state.

A. Correlation structure of ψ

ψ is normalized according to

$$\sum_Z |\psi(Z)|^2 = 1 \tag{1.2}$$

which is the statement that the classical probabilities add up to one. For classical correlators, *e.g.* $\langle Z_r Z_{r'} \rangle$, the quantum correlation function is identical to the correlation function in the classical statistical model. This is because the expectation value,

$$\sum_Z |\psi(Z)|^2 Z_r Z_{r'} = \sum_Z \frac{e^{-\beta h(Z)}}{\mathcal{Z}} Z_r Z_{r'}, \tag{1.3}$$

is manifestly given by the classical correlation function. This statement is true for any correlator consisting entirely of classical variables, *i.e.* variables in which h is diagonal. Non-classical correlations, *e.g.* $\langle X_r X_{r'} \rangle$, are more complicated.

If β corresponds to a critical temperature of the classical model h, then the classical correlations of ψ will be power law. Hence ψ necessarily describes a gapless state of matter, since gapped phases always have short-range correlations if the quantum Hamiltonian is local[42] (we will exhibit local quantum Hamiltonians whose groundstate is ψ in examples). On the other hand, the wavefunction is relatively simple and accessible, so this class of quantum states is an attractive setting to explore wavefunction RG for gapless states.

B. Entanglement structure of ψ

Even when it hosts long-range correlations, the state ψ (a square root state built from a classical statistical model with a short-ranged Hamiltonian) has no entanglement between distant regions, in the following sense. Let $|\psi\rangle = \sum_Z \psi(Z)|Z\rangle$ be the normalized quantum state and let ABC be a partition of the entire system such that B separates A from C, *e.g.* B is an annulus, A is the interior disk, and C is the rest of the world. Let $\Pi(Z_B)$ be a projector onto a state of definite Z_B (the spins in B). Then we have

$$\Pi(Z_B)|\psi\rangle = \sqrt{p(Z_B)}|\psi_A(Z_B)\rangle|Z_B\rangle|\psi_C(Z_B)\rangle, \tag{1.4}$$

or in words, fixing the state of region B causes the state of the whole system to factorize. This implies that the state ρ_{AC} is separable. In detail, writing $\rho_{ABC} \equiv |\psi\rangle\langle\psi|$, we have

$$\begin{aligned} \rho_{AC} &= \mathrm{tr}_B(\rho_{ABC}) = \sum_{Z_B} \mathrm{tr}_B(\Pi(Z_B)\rho_{ABC}\Pi(Z_B)) \\ &= \sum_{Z_B} p(Z_B)\rho_A(Z_B)\rho_C(Z_B) \end{aligned} \tag{1.5}$$

which is manifestly an incoherent mixture. Thus A and C share no entanglement and the state ρ_{AC} cannot be used to violate a Bell inequality despite the presence of long-range correlations.

By contrast, in a conformal field theory there is always some entanglement between A and C present in the ground state and a Bell inequality can be violated. This tells us that conformal field theories are not captured in the present construction.

However, we caution the reader that the Bell inequality violation and circuit notions of long-range entanglement are not equivalent. Although square root states cannot violate long-range Bell inequalities, but they can still be long-range entangled in the sense of circuits: for example, as we show later, topologically ordered states can sometimes be written as square root states. So while distant regions in the state cannot be used to violate a Bell inequality, the state is long-range entangled in the sense that it requires a high depth circuit to produce from an unentangled starting point. Indeed, the main purpose of this work is to exhibit such RG circuits.

C. Some examples

Paramagnet - The simplest possible example is where H is the Hamiltonian for a paramagnet: $H(Z) = -\sum_r Z_r$. In this case the resulting quantum wavefunction is a product state with no entanglement, but the onsite states are in a superposition of $\uparrow$: $Z = 1 \uparrow$ and $\downarrow$: $Z = -1$. The ratio of probabilities are the same as those of the classical model. The projected entangled pair states (PEPS) representation of such a state is trivial.

Ferromagnet - Another simple example occurs for the Ising model in 1d: $H(Z) = -\sum_r Z_r Z_{r+1}$. If we take the temperature $\beta = \infty$, then the resulting quantum state only has support on two configurations, all up and all down. Hence the quantum state for L spins is a cat state,

$$|\mathrm{cat}_L\rangle = \frac{1}{\sqrt{2}}(|0...0\rangle + |1...1\rangle). \tag{1.6}$$

In this equation we have switched to computational notation; 0 corresponds to ↑ and 1 corresponds to ↓, equivalently $Z = 1 - 2x$ where $x = 0$ or $x = 1$ (not to be confused with X, the Pauli matrix). This state has a matrix product (MPS[22–25]) representation

$$|h\rangle = \text{tr} \prod_i A^{\sigma_i} |\{s_i\}\rangle \tag{1.7}$$

in which the matrices may be taken to be $A^0 = |0\rangle\langle 0|$ and $A^1 = |1\rangle\langle 1|$.

A simple protocol for producing the cat state is obtained by copying in the classical basis. Start with the cat state on L sites, $|\text{cat}_L\rangle$. To make $|\text{cat}_{2L}\rangle$ introduce L spins in the state $|0\rangle$. Intercalate the unentangled spins into the entangled spins to form a chain of length $2L$ where every other spin is unentangled. Now apply L copy gates (CNOT will work) to each pair of one entangled and one unentangled spin. The copy gate performs $|00\rangle \rightarrow |00\rangle$ and $|10\rangle \rightarrow |11\rangle$. Then since the control bits are perfectly correlated it follows that the resulting state is $|\text{cat}_{2L}\rangle$.

General Ising magnet - For the bulk of the paper we focus on square root states derived from classical Ising magnetism in various dimensions. In 1d we will describe an exact RG circuit which produces the ground state while in 2d we will develop an systematic scheme to produce an approximate circuit. We will give bounds on the error of approximation using properties of the Ising magnet. The techniques we describe for the 1d and 2d Ising magnets generalize to more complicated classical statistical models.

D. Precise problem

What precisely would we like to do? Following the MERA and s-source RG framework, we would like to produce a constant depth circuit that maps the quantum state (plus initially unentangled degrees of freedom) at linear size L to the quantum state at linear size $2L$. Such a circuit succinctly captures our intuition that gapless states describe some kind of RG fixed point. We would like to make this intuition sharp and eventually tackle CFTs and even more general gapless models. A first step is to understand the long-range states arising as square root states.

The problem can be decomposed into three parts.

Module 1. The first part is purely classical: Given a statistical lattice model, identify a real-space RG scheme which produces a model of the same form on a larger lattice. This is particularly interesting for fixed-point values of the couplings. This involves (at least) two sub-modules: (1) The first is a geometric question of a re-wiring procedure on the lattice which produces the larger lattice. (2) The second is a map on the couplings for a specific model on said lattice.

Module 2. Now consider the associated quantum state on a lattice of linear size L, $|h_L\rangle$. Turn the above RG map into a unitary transformation which takes the given state (plus ancillas) to the state on a larger geometry (perhaps plus other ancillas):

$$\mathbf{U} |h_L\rangle \otimes |0...\rangle = |h_{2L}\rangle \otimes |0'...\rangle .$$

Note that it may be necessary to increase the size of the on-site Hilbert space (we will sometimes call this the 'bond dimension'), or make it infinite, to accomplish such an exact map.

Module 3. Bound the error made by truncating the bond dimension in the previous step, as a function of the bond dimension, and as a function of the range of the classical Hamiltonian h.

The payoff of this construction is an efficiently-contractible representation of the groundstate. In particular, this work provides the first non-variational circuit with quantitative error estimates for a gapless state in more than one dimension. Such a circuit is useful for analyzing strongly interacting field theories associated with quantum critical points arising from known microscopic model Hamiltonians. In the longer term, these results may shed light on the structure of quantum circuits for holographic models.

Here is a brief guide to the results in this paper. In §II, we make an RG circuit for the square root state associated to the Ising chain; although this is a degenerate case, it is an instructive warmup. In §III we implement these steps for the case of the quantum square root state for the general Ising model, focusing on two spatial dimensions. This model wavefunction exhibits several phases separated by quantum phase transitions. In §C we provide a bound on the dynamical exponent in the quantum critical point associated with the Onsager transition. In §D we provide more details about the local unitaries for this state. In §IV we discuss generalizations to other square root states, including cases where the classical model is not short-ranged.

II.   1D ISING SQUARE ROOT STATE

In this section we make a quantum circuit construction of the square root state associated with the Ising chain. Though the state in question always has a finite correlation and only short-range entanglement, the correlation length can become exponentially large as a function of βJ. Hence it is a natural toy model to begin with. Furthermore, the construction gives a clear demonstration of the capability of the RG circuit to compute useful information, such as correlation functions.

In the 1d case, the Ising square root state is:

$$|h\rangle = \frac{1}{\sqrt{\mathcal{Z}}} \sum_{\{s\}} e^{+\frac{\beta J}{2} \sum_i s_i s_{i+1}} |\{s_i\}\rangle \tag{2.1}$$

where $\mathcal{Z}$ is the partition function for 1D classical Ising model. This state is a rank 2 matrix product state

$$|h\rangle = \left(\frac{1}{\sqrt{\mathcal{Z}}}\right)^N \text{tr} \prod_i A^{\sigma_i} |\{s_i\}\rangle \tag{2.2}$$

with

$$A^\sigma = \begin{pmatrix} \cosh(\frac{\beta J}{2}) & \sigma\sqrt{\cosh(\frac{\beta J}{2})\sinh(\frac{\beta J}{2})} \\ \sigma\sqrt{\cosh(\frac{\beta J}{2})\sinh(\frac{\beta J}{2})} & \sinh(\frac{\beta J}{2}) \end{pmatrix} . \tag{2.3}$$

A parent Hamiltonian, of which this state is the ground state, is

$$H = \sum_i (-X_i + e^{-\beta J Z_i (Z_{i-1} + Z_{i+1})}) \tag{2.4}$$

The physics of this model is simple. The system is always in a paramagnetic phase where $\langle Z \rangle = 0$, but as β gets large the system develops increasingly long-ranged correlation without ever truly reaching a critical point. This is because the wavefunction is based on the 1d statistical Ising model which displays no phase transition and never supports power law correlations in the thermodynamic limit. More directly from (2.4), this is because (2.4) contains antiferromagnetic interactions between nearest neighbors and next-nearest neighbors of equal strength, and so is highly frustrated.

To verify these claims one can compute correlation functions of local operators in the ground state via transfer matrix method. In this model the transfer matrix is defined as

$$T = e^{\beta J} I + e^{-\beta J} X; \tag{2.5}$$

T is diagonalized by the unitary matrix $u = \frac{1}{\sqrt{2}}(Z + X)$, so that:

$$uTu = 2\begin{pmatrix} \cosh(\beta J) & 0 \\ 0 & \sinh(\beta J) \end{pmatrix} \tag{2.6}$$

Therefore the partition function is

$$\mathcal{Z} = 2^N (\cosh(\beta J)^N + \sinh(\beta J)^N) \tag{2.7}$$

The ZZ correlation function is

$$\begin{aligned} C^{zz}(r) &= \langle h| Z(r)Z(0) |h\rangle \\ &= \frac{\tanh(\beta J)^{N-r} + \tanh(\beta J)^r}{1 + \tanh(\beta J)^N}. \end{aligned} \tag{2.8}$$

The XX correlation function can be computed using the matrix product representation (2.2), and is

$$C^{xx}(r) = \langle h| X(r)X(0) |h\rangle = \frac{\cosh(\beta J)^{-4+N}}{\cosh(\beta J)^N + \sinh(\beta J)^N}, \tag{2.9}$$

independent of the separation, and disconnected: $\langle h| X(r)X(0) |h\rangle = (\langle h| X(0) |h\rangle)^2$.
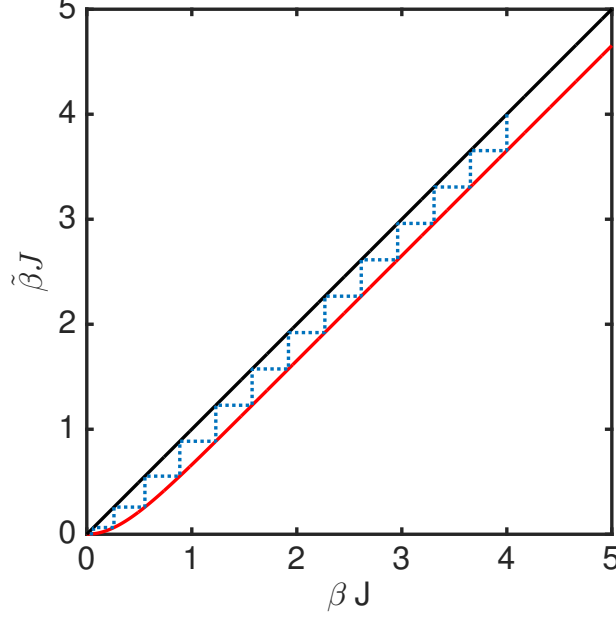
FIG. 1: Temperature flow of real space RG for 1D classical Ising model. Blue dash line represents the change of β which labels the square root state after successive RG transformation.

A. RG circuit

The 1d Ising square root state which we just introduced provides a simple exactly solvable example of an RG circuit. This is because the 1d statistical Ising model enjoys an *exact* real space renormalization group, in the sense that one can trace out half of the spin degrees of freedom in the partition function and obtain a new partition function with the same form but renormalized temperature. This procedure can be illustrated using three spins as follows:

$$
\sum_{s_i} e^{\beta J(s_{i-1}s_i + s_i s_{i+1})}
$$
$$
= e^{\beta J(s_{i-1}+s_{i+1})} + e^{-\beta J(s_{i-1}+s_{i+1})} \tag{2.10}
$$
$$
= 2\sqrt{\cosh(2\beta J)} e^{\frac{1}{2}\ln\cosh(2\beta J)s_{i-1}s_{i+1}}
$$

Therefore the renormalized temperature (Fig. 1) is:

$$
\tilde{\beta}J = \frac{1}{2}\ln\cosh(2\beta J) . \tag{2.11}
$$

There are two fixed points: the unstable low temperature fixed point and the stable high temperature fixed point. Therefore, under the RG flow, the classical Ising model, if not completely ordered, eventually flows to a completely disordered phase.

Now let us explore the resulting RG circuit in the quantum theory. We first discuss the RG transformation of the state (Eq. (2.1)) then the Hamiltonian (Eq. (2.4)). In the state, a single site spin state is completely determined once its neighboring spin states are fixed, and we have the freedom to apply a local unitary transformation to transform this spin state into an arbitrary state we desire. Consider a subset of three spins in the whole chain with the left and right spins fixed:

$$
|\psi_i^{s_{i-1}s_{i+1}}\rangle = \sum_{s_i} e^{\frac{\beta J}{2}(s_{i-1}s_i + s_i s_{i+1})} |s_{i-1}s_i s_{i+1}\rangle . \tag{2.12}
$$

For arbitrary s_{i-1} and s_{i+1}, there exists a *single* unitary operator U_i that disentangles the middle qubit with its neighbors by converting it to the eigenstate of X_i with the positive eigenvalue, denoted as $|\rightarrow\rangle_i$.

$$
U_i |\psi_i^{s_{i-1}s_{i+1}}\rangle = \sqrt{2}\cosh^{\frac{1}{4}}(2\beta J)e^{\frac{\tilde{\beta}J}{2}s_{i-1}s_{i+1}} |s_{i-1}s_{i+1}\rangle \otimes |\rightarrow_i\rangle \tag{2.13}
$$

The explicit form of U_i is:

$$U_i = \sum_{s_l, s_r} \mathcal{P}_{i-1}^{s_l} u_i^{s_l, s_r} \mathcal{P}_{i+1}^{s_r} \tag{2.14}$$

$\mathcal{P}_i^s$ is a projection operator $\frac{1}{2}(I_i + sZ_i)$ and $u_i^{s_l s_r}$ is an on-site unitary operator depending on s_l and s_r:

$$u_i^{s_l s_r} = \frac{\delta^{s_l s_r}}{\sqrt{\cosh(2\beta J)}} \left((\cosh(\beta J) - 1)I_i - \mathbf{i}s_l \sinh(\beta J)Y_i\right) + I_i \tag{2.15}$$

Then $U \equiv \prod_{i \in odd} U_i$ puts all spins on odd sites into a product state of spin right and converts all even sites spins into a new Ising square root state with the renormalized temperature $\tilde{\beta}$ (Fig. 1):

$$U \left| h \right\rangle = \prod_{i \in \text{odd}} u_i \left| h(\beta) \right\rangle = \left| h\left(\tilde{\beta}, \text{even}\right) \right\rangle \otimes \prod_{i \in \text{odd}} \left| \rightarrow_i \right\rangle . \tag{2.16}$$

The U_i with i odd commutes with each other, therefore U is also unitary. After this unitary transformation, the even site spins and odd site spins are completely disentangled with each other. Furthermore, the odd site spins are in a product state. When we repeatedly apply the above RG circuit, β for the new square root state approaches zero and the unitary transformation approaches the identity. As a result, we obtain a product of all spin-right states, which is the stable fixed point of this unitary RG transformation, depicted in Fig. 2 as a circuit. Expectation values of any operators $\mathcal{O}$ in the ground state can be written in the following form:

$$\langle h | \mathcal{O} | h \rangle = \langle X | ... U^{(2)} U^{(1)} \mathcal{O} U^{(1),\dagger} U^{(2),\dagger} ... | X \rangle \tag{2.17}$$

where $|X\rangle$ is just the product of spin-right state. Now we demonstrate how to use our RG circuit to compute the above quantity. In the case that $\mathcal{O}$ has a support of a single site i, it is easier to start by putting $\mathcal{O}$ under a unitary transformation (green triangle). Applying U once, $\mathcal{O}$ only affects the unitary transformation and two adjacent controllers, and other part of the circuit at this layer can be efficiently contracted. We obtain a two site operator which is purely composed of projection operator in the next layer. Since the unitary transformation later on does not effect site i anymore, we are ready to compute its expectation value, which is just a number entering the next layer. Putting the words above into equations, we have

$$\begin{aligned} \tilde{\mathcal{O}}^{(1)} &= \langle \rightarrow_i | U_i \mathcal{O} U_i^{\dagger} | \rightarrow_i \rangle \\ &= \sum_{s_l, s_r} \mathcal{P}_{i-1}^{s_l} \langle \rightarrow | u_i^{s_l s_r} \mathcal{O} u_i^{s_l s_r, \dagger} | \rightarrow \rangle \mathcal{P}_{i+1}^{s_r} \\ &= \sum_{\alpha\beta} \mathcal{P}_{i-1}^{\alpha} m^{\alpha\beta} \mathcal{P}_{i+1}^{\beta} \end{aligned} \tag{2.18}$$

where $m^{\alpha\beta} = \langle \rightarrow | u_i^{\alpha\beta} \mathcal{O} u_i^{\alpha\beta, \dagger} | \rightarrow \rangle$. The superscript (1) stands for the operator after applying U once, which has the support on site $i-1$ and site $i+1$. Fig. 3 (a) is a graphic representation of the formula above. If we apply the transformation again, there are two possible cases illustrated in Fig. 3 (b). Either way, we retain an operator with the same form but with m replaced by a new $\tilde{m}$.

More explicitly, the first case:

$$\mathcal{O}_1^{(2)} = \sum_{\alpha\beta\gamma} \mathcal{P}^{\alpha} m^{\alpha\gamma} \langle \rightarrow | u^{\alpha\beta} \mathcal{P}^{\gamma} u^{\alpha\beta\dagger} | \rightarrow \rangle \mathcal{P}^{\beta} \tag{2.19}$$

The second case:

$$\mathcal{O}_2^{(2)} = \sum_{\alpha\beta\gamma} \mathcal{P}^{\alpha} m^{\gamma\beta} \langle \rightarrow | u^{\alpha\beta} \mathcal{P}^{\gamma} u^{\alpha\beta\dagger} | \rightarrow \rangle \mathcal{P}^{\beta} \tag{2.20}$$

After averaging both cases, we obtain:

$$\tilde{m}^{\alpha\beta} = \sum_{\gamma} \frac{1}{2} \langle \rightarrow | u^{\alpha\beta} \mathcal{P}^{\gamma} u^{\alpha\beta\dagger} | \rightarrow \rangle (m^{\alpha\gamma} + m^{\gamma\beta}) \tag{2.21}$$
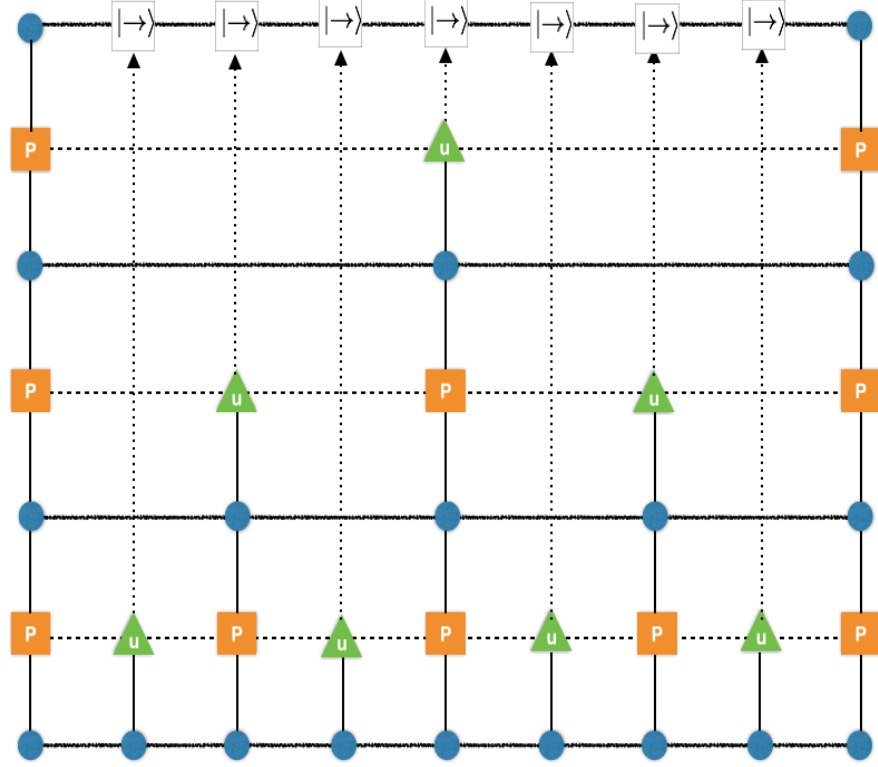
FIG. 2: Sketch of the RG circuit for the quantum Ising chain. The blue dots in the bottom layer represent the initial square root state. Green triangles are unitary operators $u_i^{s_l s_r}$ (Eq. 2.15) and yellow squares are projection operators $\mathcal{P}_i^s$, serving as controllers. Horizontal dash lines contract the indices. After each iteration, the state on the odd sites become product state $|X\rangle$, and distangled from the state on the even sites which forms a new square root state with renormalized β. Eventually, the initial state is transformed by local unitary operators to a complete untangled state $|X\rangle$ (top layer).

If we obtain $m^{(n)}$ in the end of the unitary-RG transformation, then the targeted expectation value is:

$$\langle \mathcal{O} \rangle = \frac{1}{4} \sum_{\alpha\beta} m^{(n),\alpha\beta} \tag{2.22}$$

All the information about the operator we are coarse-graining is encoded in the initial value of m. Writing down each component of Eq. 2.21, we have:

$$
\begin{aligned}
\tilde{m}^{11} &= \frac{1}{4}(2(1 + \tanh(2\beta J))m^{11} + (1 - \tanh 2\beta J)(m^{12} + m^{21})) \\
\tilde{m}^{12} &= \frac{1}{4}(m^{11} + 2m^{12} + m^{22}) \\
\tilde{m}^{21} &= \frac{1}{4}(m^{11} + 2m^{21} + m^{22}) \\
\tilde{m}^{22} &= \frac{1}{4}(2(1 + \tanh(2\beta J))m^{22} + (1 - \tanh 2\beta J)(m^{21} + m^{12}))
\end{aligned}
\tag{2.23}
$$

With Eq. 2.11, this set of equations completely defines an iteration procedure from the initial operator to the final
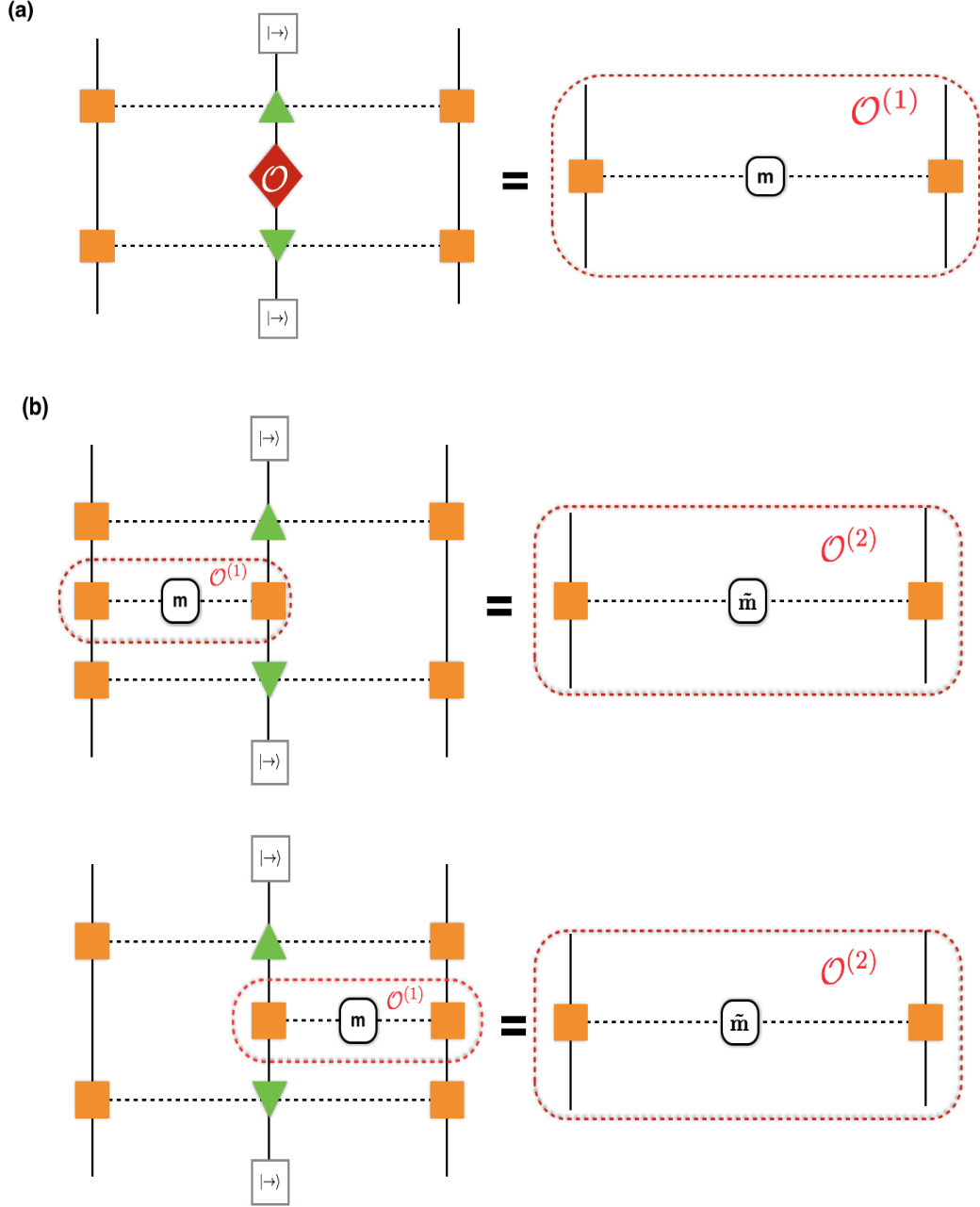
FIG. 3: Transformation of a single site operator under unitary-RG transformation. Green triangles are unitary operators $u_i^{s_l s_r}$ and yellow squares are projection operators $\mathcal{P}_i^s$, serving as controllers. Dash lines contract the indices. (a) The application of $U^{(1)}$ on a local operator $\mathcal{O}$ (red diamond) that has its support on a single site. After the transformation, the renormalized new operator, denoted as $\mathcal{O}^{(1)}$ has its support on two sites, in the form of two projection operators linked by a matrix m determined by the initial operator $\mathcal{O}$. (b) We apply unitary transformation $U^{(2)}$ to $\mathcal{O}^{(1)}$. The middle site in (a) is omitted since it is disentangled with the rest of the Hilbert space. There are two equivalent situations. In the first case, $u^{s_l s_r}$ is applied to the right projection operator in $\mathcal{O}^{(1)}$; in the second case, $u^{s_l s_r}$ is applied to the left projection operator. After the transformation, a new operator $\mathcal{O}^{(2)}$ is obtained, which shares the same form as $\mathcal{O}^{(1)}$ but with renormalized $\tilde{m}$. Then this procedure can be repeated.

fully renormalized operator. The eigenvalues and eigenvectors for a single iteration of the mapping are:

$$E = \begin{pmatrix} 1 & \frac{1}{2}(1 + \tanh(2\beta J)) & \frac{1}{2} & \frac{1}{2}\tanh 2\beta J \end{pmatrix}$$

$$V = \begin{pmatrix} 1 & -1 & 0 & 1 \\ 1 & 0 & -1 & -\frac{1}{1-\tanh(2\beta J)} \\ 1 & 0 & 1 & -\frac{1}{1-\tanh(2\beta J)} \\ 1 & 1 & 0 & 1 \end{pmatrix} \tag{2.24}$$

Now we discuss behavior of the Hamiltonian under this unitary-RG transformation. Expanding the exponential in Eq. 2.4, the Hamiltonian is a transverse field model with next neighboring interaction:

$$H = -\sum_i X_i - \sinh(2\beta J) \sum_{\langle i,j \rangle} Z_i Z_j$$
$$+ \sinh^2(\beta J) \sum_{\langle\langle i,j \rangle\rangle} Z_i Z_j + N \cosh^2(\beta J) \tag{2.25}$$

To obtain the new Hamiltonian, the strategy is to feed each term into our RG circuit while fixing the ancillary degree freedom into its ground state, namely all spin right. To make it clear, we assume that all ancillas are at even sites and the physical degrees of freedom are at odd sites. Therefore for the X_i term, there are two cases: even i and odd i, the renormalized form of which are different. For the first case:

$$X_{2m+1} \to \mathcal{P}_{2m}^\alpha \langle\to| u_{2m+1}^{\alpha\beta} X_{2m+1} u_{2m+1}^{\alpha\beta\dagger} |\to\rangle \mathcal{P}_{2m+2}^\beta$$
$$= \left(\frac{1}{\cosh(2\beta J)} - 1\right)(\mathcal{P}_{2m}^\uparrow \mathcal{P}_{2m+2}^\uparrow + \mathcal{P}_{2m}^\downarrow \mathcal{P}_{2m+2}^\downarrow) + 1 \tag{2.26}$$

The second case is more involved:

$$X_{2m} \to \mathcal{P}_{2m-2}^\alpha \langle\to| u_{2m-1}^{\alpha\beta} u_{2m-1}^{\alpha\gamma\dagger} |\to\rangle \mathcal{P}_{2m}^\beta X \mathcal{P}_{2m}^\gamma$$
$$\langle\to| u_{2m+1}^{\beta\delta} u_{2m+1}^{\gamma\delta\dagger} |\to\rangle \mathcal{P}_{2m+2}^\delta$$
$$= \frac{\cosh^2(\beta J)}{\cosh(2\beta J)} X_{2m} \tag{2.27}$$

The transformation of the nearest neighboring interaction also has two cases, but it turns out that the two cases are identical:

$$Z_{2m-1} Z_{2m} \to \mathcal{P}_{2m-1}^\alpha Z_{2m-1} \langle\to| u_{2m}^{\alpha\beta} Z_{2m} u_{2m}^{\alpha\beta\dagger} |\to\rangle \mathcal{P}_{2m+1}^\beta$$
$$= \tanh(2\beta J)(\mathcal{P}_{2m-1}^\uparrow \mathcal{P}_{2m+1}^\uparrow + \mathcal{P}_{2m-1}^\downarrow \mathcal{P}_{2m+1}^\downarrow)$$
$$Z_{2m} Z_{2m+1} = \tanh(2\beta J)(\mathcal{P}_{2m-1}^\uparrow \mathcal{P}_{2m+1}^\uparrow + \mathcal{P}_{2m-1}^\downarrow \mathcal{P}_{2m+1}^\downarrow) \tag{2.28}$$

The contribution of the two cases should add up and give an extra factor of 2. Last we need study the transformation of the next neighboring interaction, which, as same as before has two cases. The first one:

$$Z_{2m} Z_{2m+2} \to \mathcal{P}_{2m}^\alpha Z_{2m} \mathcal{P}_{2m+2}^\beta Z_{2m+2}$$
$$= 2(\mathcal{P}_{2m}^\uparrow \mathcal{P}_{2m+2}^\uparrow + \mathcal{P}_{2m}^\downarrow \mathcal{P}_{2m+2}^\downarrow) - 1 \tag{2.29}$$

The second one:

$$Z_{2m-1} Z_{2m+1} \to \mathcal{P}_{2m-2}^\alpha \langle\to| u_{2m-1}^{\alpha\beta} Z_{2m-1} u_{2m-1}^{\alpha\beta\dagger} |\to\rangle$$
$$\mathcal{P}_{2m}^\beta \langle\to| u_{2m+1}^{\beta\gamma} Z_{2m+1} u_{2m+1}^{\beta\gamma\dagger} |\to\rangle \mathcal{P}_{2m+2}^\gamma$$
$$= \tanh^2(2\beta J)(\mathcal{P}_{2m-2}^\uparrow \mathcal{P}_{2m}^\uparrow \mathcal{P}_{2m+2}^\uparrow + \mathcal{P}_{2m-2}^\downarrow \mathcal{P}_{2m}^\downarrow \mathcal{P}_{2m+2}^\downarrow) \tag{2.30}$$

Although these two terms look like they involve interactions between three Zs, they actually cancel each other, which is a necessary consequence of the $\mathbb{Z}_2$ symmetry. After carefully organizing all the terms above, and converting β into the renormalized $\tilde{\beta}$, one can find that the resultant Hamiltonian has the exact same form as it in Eq. 2.4 with an overall constant $\frac{1}{2}e^{-2\tilde{\beta}J}(1 + e^{-2\tilde{\beta}J})$.

III. 2D ISING SQUARE ROOT STATE

Having studied in detail the RG circuit for the square root state of the 1d statistical Ising model, we now turn to a construction of the RG circuit for the square root state associated with the 2d statistical Ising model. To carry out Module 1 for this model we will use a specific implementation of the real-space RG due to Levin and Nave[26]. This procedure is already enough to give interesting results, so we focus on it for simplicity, but our considerations are sufficiently modular that they can be carried out for various extensions and generalizations of the original scheme.[43]

To set up the model, put qubits on the links of the honeycomb lattice, and label a basis by $|s\rangle$, eigenstates of Pauli operators Z_i on the links, $Z_i|s\rangle = s_i|s\rangle$. Consider the following square root state:

$$|\psi_T\rangle = \frac{1}{\sqrt{\mathcal{Z}}}\sum_{\{s\}}|s\rangle\,\sqrt{T_{s_1s_2s_3}T_{s_3s_4s_5}...} \tag{3.1}$$

with $\mathcal{Z} \equiv \sum_{\{s\}} TT...$ the associated classical partition function. As explained in[26], if we take $T_{+++} = 1, T_{--+} = T_{+--} = T_{+--} = e^{-2\beta J}$ (and other components of the tensor, which would describe domain walls which end, are zero) this is the Ising model on the triangular lattice (up to a factor of two in $\mathcal{Z}$), where the two link configurations represent: $+ \equiv$ "no domain wall" and $- \equiv$ "yes domain wall". To turn on a magnetic field in the Ising model (necessary to compute for example the magnetization) requires a complication of this scheme which we do not write out explicitly.

Consider the state associated with the Ising model on any graph

$$|h\rangle \equiv \frac{1}{\sqrt{\mathcal{Z}}}\sum_{\{s\}}e^{+\frac{\beta J}{2}\sum_{\langle ij\rangle}s_is_j}|\{s\}\rangle. \tag{3.2}$$

(Note that we have chosen the normalization $h(s) = -J\sum_{\langle ij\rangle}s_is_j$ so that $J > 0$ gives a ferromagnetic classical ising model.)

Acting on qubits at the sites of any graph (not just 2d lattices), consider:

$$\mathbf{H} \equiv \sum_i c_i(\beta)\left(-X_i + e^{-\beta JZ_i\sum_{\langle i|j\rangle}Z_j}\right)\quad. \tag{3.3}$$

The notation $\langle i|j\rangle$ means "the set of neighbors j of the fixed site i". $c_i(\beta)$ are positive coupling constants the choice of which is discussed in §B.

The state $|h\rangle$ in (3.2) is the groundstate of $\mathbf{H}$. First of all, it is an eigenvector with eigenvalue zero, $\mathbf{H}|h\rangle = 0$. In a little more detail,

$$
\begin{aligned}
X_i|h\rangle &= \frac{1}{\sqrt{\mathcal{Z}}}\sum_{\{\tilde{s}_j\equiv s_j,j\neq i,\tilde{s}_i\equiv -s_i\}}e^{\frac{\beta}{2}\sum_{\langle ij\rangle}s_is_j}|\{\tilde{s}\}\rangle\\
&= \frac{1}{\sqrt{\mathcal{Z}}}\sum_{\{\tilde{s}\}}e^{-\beta\sum_{\langle i|j\rangle}\tilde{s}_i\tilde{s}_j}e^{+\frac{\beta}{2}\sum_{\langle ij\rangle}\tilde{s}_i\tilde{s}_j}|\{\tilde{s}\}\rangle\\
&= e^{-\beta JZ_i\sum_{\langle i|j\rangle}Z_j}|h\rangle.
\end{aligned} \tag{3.4}
$$

Secondly, $\mathbf{H}$ is positive, so the zero eigenvector is the groundstate. In the sum over sites in $\mathbf{H}$, each term H_i is an operator with eigenvalues greater than or equal to zero. This is because H_i is block diagonal in the Z basis for the neighbors; in the block where $\sum_{\langle i|j\rangle}Z_j \equiv S$, it is $H_i = -X_i + e^{-\beta JSZ_i}$ which has eigenvalues $0, 2\cosh\beta JS$. The eigenvalues of $\mathbf{H}$ itself are therefore bounded below by zero. (This is an application of the Perron-Frobenius theorem.)

The physics of this model is more interesting than the corresponding 1d model. Here there are two phases, a paramagnetic phase at small β and a ferromagnetic phase at large β. These phases are separated by a quantum critical point describing a symmetry breaking transition which is however not the usual Wilson-Fisher fixed point (it is not even conformally invariant). Because the exact critical point of the 2d statistical Ising model is known (on the honeycomb lattice, for example, it is $(\beta J)_\star \simeq 0.658$ (e.g.[33])) we know the exact location of the critical point in the square root state model. We know this must be a quantum critical point because the Hamiltonian is local but correlation functions of local operators, for example, Z_j, become long-ranged at this point. This critical point is a non-trivial interacting fixed point which is multicritical, meaning it has more than one relevant symmetry-preserving perturbation. We say this because we know that the ordinary $z = 1$ Wilson-Fisher fixed point also lies on the same phase boundary between paramagnetic and ferromagnetic phases.

We note that it will be interesting to build a field theory description of this fixed point. Such a description will almost certainly involve strong coupling, so the existence of an RG circuit that can be used to compute operator dimensions will be a powerful tool in analyzing the field theory. At the same time, the field theory will give us more information about the dynamical properties of the quantum critical point. The two approaches are complementary. We are currently searching for a field theory description, e.g. by continuing the dimensionality away from 2 in an ϵ expansion.

A. RG circuit

The RG step has two parts. The first part is a channel-duality rewiring move, and the second is the coarse-graining step. In fact, both steps will involve ancilla qubits.

Let $\mathcal{H}_a$ denote the single-qubit Hilbert space of a. The first step should be made of local unitaries which act by

$$U_1 : \mathcal{H}_{abcd} \otimes \mathcal{H}_e \otimes \mathcal{H}_f \rightarrow \mathcal{H}_{abcd} \otimes \mathcal{H}_e \otimes \mathcal{H}_f \tag{3.5}$$

We require:

$$U_1 \left| \begin{array}{c} a \\ b \end{array} \!\!\! \rangle\!\!\!\!\!< \begin{array}{c} c \\ d \end{array} \right\rangle \otimes |0\rangle_f = \sum_f \left| \begin{array}{c} a \\ b \end{array} \!\!\! \rangle\!\!\!\! f \!\!\!\!< \begin{array}{c} c \\ d \end{array} \right\rangle \otimes |0\rangle_e \tag{3.6}$$

or in more explicit notation,

$$U_1 \sum_{abcde} \sqrt{T_{abe}T_{ecd}} \, |abcde\rangle \otimes |0\rangle_f$$
$$= \sum_{abcdf} \sqrt{S_{acf}S_{fbd}} \, |abcd\rangle \, |0\rangle_e \otimes |f\rangle_f \ . \tag{3.7}$$

Note that this rewiring move involves both adding and subtracting ancillas. Before the action of U_1, the ancillary Hilbert space $\mathcal{H}_f$, is disentangled from $\mathcal{H}_{abcd} \otimes \mathcal{H}_e$ in the groundstate. U_1 entangles $\mathcal{H}_f$ with $\mathcal{H}_{abcd}$, but disentangles $\mathcal{H}_e$. As a result, $\mathcal{H}_f$ becomes part of the physical space, while $\mathcal{H}_e$ becomes ancillary. To accomplish this, it suffices to take

$$U_1 \sum_e \sqrt{T_{abe}T_{ecd}} \, |abcde\rangle \otimes |0\rangle_f = \sum_f |abcd0f\rangle \sqrt{S_{acf}S_{fbd}} \tag{3.8}$$

Notice that the preceding equation does not define the action of U_1 on a general basis state.

As we demonstrate in §D, the classical RG relation

$$\sum_e T_{abe}T_{ecd} = \sum_f S_{acf}S_{fbd} \tag{3.9}$$

is just what is needed to imply that U_1 is norm-preserving.

The second step is implemented by

$$U_2 \left| \begin{array}{c} k \quad j \\ \mathsf{Y} \\ i \end{array} \right\rangle \otimes |000\rangle = \sum_{abc} \left| \begin{array}{c} k \!\! \stackrel{c}{\diagdown}\!\! j \\ a\mathsf{Y}b \\ i \end{array} \right\rangle \tag{3.10}$$

The requirement is:

$$U_2 \sum_{ijk} \sqrt{T_{ijk}T_{i..}T_{j..}T_{k..}} \, |ijk\rangle \otimes |000\rangle$$
$$= \sum_{ijkabc} \sqrt{S_{iab}S_{jbc}S_{kac}T_{i..}T_{j..}T_{k..}} \, |ijkabc\rangle \tag{3.11}$$

for all values of the un-named indices. To accomplish this, it is sufficient simply to set

$$U_2 \, |ijk000\rangle = \sum_{abc} |ijkabc\rangle \sqrt{\frac{S_{iab}S_{jbc}S_{kac}}{T_{ijk}}} . \tag{3.12}$$

(The RHS is understood to be zero if any of the S_{iab} vanish.) Note that the relation

$$\sum_{abc} S_{iab} S_{jbc} S_{kac} = T_{ijk} \tag{3.13}$$

implies that U_2 defined by this equation preserves the norm, as shown in §D.

We note that the conditions (3.8) and (3.11) do not completely specify $U_{1,2}$, since they do not determine the action on excited states. This is a useful freedom which merits further exploration.

The resulting unitary gates are depicted in Fig. 4.

B.   Truncation

The procedure just outlined can *exactly* capture the critical point of the model if and only if an infinite bond dimension is used. However, we will show that a truncation to a rather modest bond dimension – polynomial in system size – is sufficient to guarantee high overlap with the true ground state in the thermodynamic limit. We need two crucial facts: (1) the scaling of entanglement in the quantum state described by the statistical model with boundary is logarithmic in subsystem size and (2) the particular sparse and conditional structure of the RG circuit produced above makes it easy to truncate the circuit while preserving unitarity.

Following[26], consider a large triangular region of the lattice, whose side lengths are L. A sequence of coarse-graining maps on the wavefunction reduces the product of tensors in this region to a single tensor with one index for each side of the triangle. Fixing the values of the indices at the boundary of the region, this product approaches (at large L) the groundstate wavefunction of a 1d quantum system – in the example on which we focus, it is the 1d transverse-field Ising model (TFIM). Away from criticality, the mth eigenvalue of the reduced density matrix of a subregion falls off like $e^{-c \log^2 m}$ for some constant c; this holds as long as the subregion is much larger than the correlation length. This falloff accounts for the favorable convergence of the TRG away from the critical point[26].

But even at criticality, the situation is not so dire. The reduced density matrix for the state of the 1d quantum system on each side of the triangle has an eigenvalue distribution which is well-peaked about $\log(\lambda) = -S$, where S is its von Neumann entropy[34,35]. Therefore, there exists a number k of order one such that truncating the infinite bond dimension to e^{kS} states incurs only a small error of order e^{-S}. For the groundstate of the critical TFIM, a 1d CFT with central charge $c = 1/2$, the entanglement entropy of an interval of length L behaves as $S(L) = \frac{c}{3} \log L$[36]. Thus with a truncated bond dimension of size e^{kS}, that is polynomial in L, the error in our approximation to the groundstate of the large triangle goes like $e^{-S} = L^{-c/3}$. Note that the argument was put in the context of the Ising model, but it holds for any CFT provided we take the appropriate central charge.

It is also important that the truncated circuit with bond dimension e^{kS} is still composed of unitary operators. The crucial conditions are (3.9) and (3.13), which must be satisfied with the summations running over the appropriate finite bond dimension.

The conditions (3.9) and (3.13) can be solved numerically with arbitrary β, using various bond dimensions, as in[26]. The approximate circuit can then be used to learn about scaling dimensions and operator product expansion coefficients of a strongly interacting quantum critical point described by Eq. 3.3. This is a non-trivial calculation which we plan to explore in future work; it will also be desirable to compare these calculations with field theory computations if an appropriate field theory can be constructed.

C.   Topologically ordered phase

In fact, the Ising models we have been considering, when placed on the right kind of lattice, can describe even more interesting phases. This will allow us to make contact with previous literature on exact RG circuits[37,38].

On any bipartite lattice a sublattice rotation $Z_i \to (-1)^i Z_i$ relates $J > 0$ to $J < 0$ for the $e^{-\beta J Z_i \sum Z_j}$ term of (3.2), just as it relates ferromagnetic and antiferromagnetic (AFM) statistical Ising models. But on a non-bipartite lattice there is something different at $J < 0$. In the state associated with a classical frustrated magnet, there are many terms in the superposition with the same weight. This is a symptom of topological order. In particular, there is a map from the triangular lattice AFM to the honeycomb lattice dimer model: the domain walls on the honeycomb lattice form closed loops which should be regarded as *differences* of dimer configurations. (For a summary of this mapping, see appendix A of[17] and[16].)

Consider quantum spins on the triangular lattice. States which are minima of the local antiferromagnetic Heisenberg interaction have one link of each triangle in a singlet. Such states can be mapped to dimer coverings (every site covered by exactly one dimer) of the dual (honeycomb) lattice just by covering the links which intersect the singlets. The
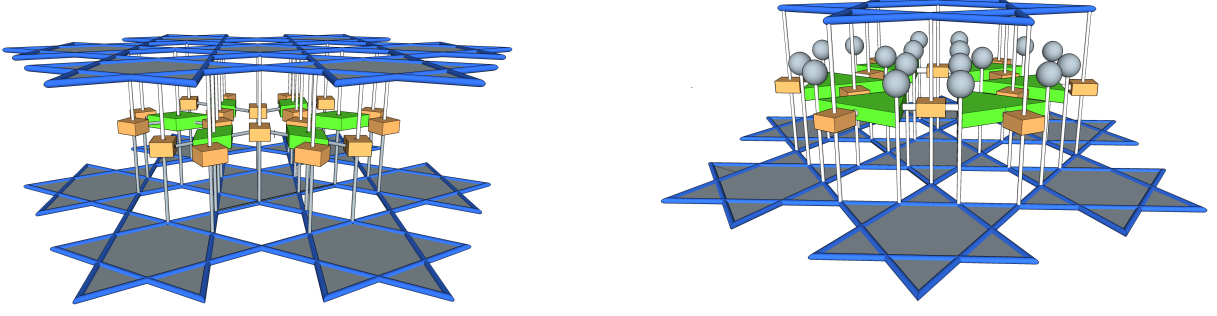
FIG. 4: A sketch of the ingredients of the RG circuit for a 2d quantum Ising square root state. In the TRG representation of the triangular lattice Ising model, the tensors act on vector spaces associated with the links of the lattice; we have found it convenient to draw directly the resulting link lattice, which in this case is the Kagome lattice. The rewiring step U_1 is at left and the disentangling step U_2 is at right. Orange blocks are controllers, green blocks are unitary transformations that depend on the controllers that connected to them. White balls represent disentangled sites. This color choice is consistent with the figures above for the one-dimensional case.

uniform superposition of these states is closely related to the state we get in the limit $\beta \to \infty, \beta J < 0$. The only difference is that instead of singlets, we have $|\uparrow\downarrow\rangle + |\downarrow\uparrow\rangle$ – all positive coefficients – on the dimer-covered links. This difference is of the form described in §IV, taking advantage of the ambiguity in the phase of the square root. So this limit gives exactly the Rokhsar-Kivelson state[15].

Since $\beta = 0$ is a paramagnet there must be another phase transition in between at negative J.

In the limit $\beta \to \infty, \beta J < 0$, the construction above is exact, with finite bond dimension. In particular, the tensors simplify dramatically: with the labelling where the index i counts the number of domain walls on the associated link ($i = 0$ or 1), we have $T_{ijk} = \delta_{i+j+k}$, where the argument of the Kronecker delta is to be understood modulo two: it merely enforces that the domain walls are closed loops.

The resulting circuit is self-dual under channel duality:

$$\sum_{k=0}^{1} T_{ijk} T_{klm} = \sum_{n=0}^{1} T_{iln} T_{njm} \tag{3.14}$$

– that is $S = T$. In this limit, the rewiring move

$$U_1 \left| \begin{smallmatrix} a \\ \\ b \end{smallmatrix} \middle\rangle \kern-0.5em \middle\langle \begin{smallmatrix} c \\ \\ d \end{smallmatrix} \right\rangle \otimes |0\rangle_f = \sum_f \left| \begin{smallmatrix} a & c \\ f \\ b & d \end{smallmatrix} \right\rangle \otimes |0\rangle_e \tag{3.15}$$

is accomplished by $U_1 = CX_{ae}CX_{be}CX_{af}CX_{cf}$, where the control-X gate is $CX_{12} \equiv \sum_{s_1} |s_1\rangle \langle s_1| \otimes X_2^{s_1}$. This is a result of[37]. Similarly, the decimation move

$$U_2 \left| \begin{smallmatrix} k & & j \\ & \\ & i \end{smallmatrix} \right\rangle \otimes |000\rangle = \sum_{abc} \left| \begin{smallmatrix} k & c & j \\ a & b \\ & i \end{smallmatrix} \right\rangle \tag{3.16}$$

is accomplished by

$$U_2 = CX_{kc}CX_{jc}CX_{ib}CX_{ab}CX_{ia}CX_{ka} \ . \tag{3.17}$$

These specific formulae are consistent with the demands we put on our circuit.

IV. DISCUSSION

In this paper we have provided examples of quantum critical groundstates in various dimensions which satisfy an area law and which have high-fidelity tensor network representations with favorable (polynomial in system size) bond dimensions. Some of our examples represent rigorous constructions of RG circuits for scale invariant states of matter in more than one dimension, a significant step forward in our understanding of wavefunction RG. There are several immediate directions for further work.

First, the quantum critical point described by Eq. 3.3 at the Ising transition should be characterized more precisely. One part of the analysis will be a detailed study of the RG circuit we constructed in this paper. Data that should be extracted include scaling dimensions and operator product expansion coefficients. Such a study should also take advantage of the fact that thermal states of Eq. 3.3 can be efficiently simulated using Monte Carlo methods (because all off-diagonal matrix elements are non-positive). It will also be desirable to incorporate a field theory analysis of the critical point.

Second, we anticipate that it is possible to go beyond our results to system-size independent bond dimension using the tensor network renormalization introduced in[30]. It should also be possible to construct quasi-local RG circuits which perform an exact RG transformation. Our constructions are generalizable to higher dimensions once the appropriate classical RG transformations are employed. A particularly interesting question is the issue of truncation of the tensors.

Third, it would be very desirable to extend our results to conformal field theories. One idea for progress is to use the fact that the free boson CFT has a wavefunction which is a square root state corresponding to a non-local statistical weight. If it could be shown that there existed a local RG transformation (which exists on physical grounds) despite the non-locality, then we would have an RG circuit for at least one CFT in higher dimensions. As a first step, in appendix A, we formulate square root states for classical models with long-range interactions.

In the rest of this concluding section, we briefly discuss other directions in which one might apply the technology developed here.

Quantum Lifshitz theories and generalizations

It is not necessary that the configuration space of the classical model be discrete. For example, it may be a continuum field theory. We recall the structure of the "Lifshitz theories" described in[18] (and more recently studied in[19]) where the statistical mechanics model in question is a Gaussian free field. In particular, there we have states labelled by a configuration of a scalar field $\phi(x)$. (The continuum is not so crucial, but the notation is less dependent on detailed lattice conventions.)

$$|h\rangle = \int [D\phi]\,|\phi\rangle\,e^{-\frac{1}{2}\int d^d x (\nabla\phi)^2} \equiv \int [D\phi]\,|\phi\rangle\,\Psi[\phi]. \tag{4.1}$$

Since

$$-\frac{\delta}{\delta\phi(x)}\Psi[\phi] = +\frac{\delta}{\delta\phi(x)}\int d^d x (\nabla\phi)^2\Psi[\phi] = -\nabla^2\phi(x)\Psi[\phi] \tag{4.2}$$

the wavefunction satisfies

$$\left(-\left(\frac{\delta}{\delta\phi(x)}\right)^2 + \left(\nabla^2\phi\right)^2\right)\Psi[\phi] = 0. \tag{4.3}$$

Since the operator

$$\mathbf{H} \equiv \int d^d x \left(\pi(x)^2 + \left(\nabla^2\phi(x)\right)^2\right) \tag{4.4}$$

(here $\pi(x)$ is the canonical field momentum, $[\phi(x), \pi(y)] = i\delta^d(x-y)$) is positive, the state $|h\rangle$ with eigenvalue zero is its groundstate.

More generally, it's not so important that the classical h be quadratic. We could replace $\int(\nabla\phi)^2$ with any real local functional $S[\phi]$ and the state

$$|S\rangle = \int [D\phi]\,|\phi\rangle\,e^{-S[\phi]} \tag{4.5}$$

is the groundstate of

$$\mathbf{H}_S \equiv \int d^d x \left(\pi(x)^2 + \left(\frac{\delta S}{\delta\phi(x)}\right)^2 + \frac{\delta^2 S}{\delta\phi(x)^2}\right). \tag{4.6}$$

Multiple roots

Our construction has numerous extensions. For example: as always, there is more than one square root. Since $\langle s|s'\rangle = \delta_{ss'}$, we can multiply each basis state $|s\rangle$ by an s-dependent phase without losing the defining property that correlators of Z-basis operators in the state are given by the classical model.

So a much larger class of square root states is of the form

$$|h, \phi\rangle \equiv \frac{1}{\sqrt{Z}} \sum_s e^{-\frac{1}{2}\beta h(s)} e^{i\phi(s)} |s\rangle \tag{4.7}$$

where ϕ is any real function on the statistical mechanics configuration space.

Positivity of the wavefunction at $\phi = 0$ is useful for application of the Frobenius theorem, and in general this is lost for $\phi \neq 0$. These states can certainly be orthogonal to $|h, \phi = 0\rangle$.

Correlation functions of Zs are independent of ϕ, because the absolute value removes this phase from each term of the sum. However, correlations of off-diagonal operators involving Xs will depend on ϕ.

This suggests a further generalization: we may consider square root states of partition functions which are sums of complex weights. Such sums arise for example in the euclidean path integral formulation of quantum systems with nontrivial Berry phases.

Dynamics

While most of this paper has focussed on groundstate properties, of course dynamics are interesting too. The frustration-free construction we have employed means we don't learn that much about dynamics from the groundstate. In particular, there are many local Hamiltonians with this same groundstate, but different spectra of excited states away from criticality. (For every such choice, the gap must close at the critical point.)

However, we can say something about the dynamics for some natural choice of the Hamiltonian, as we describe in appendix C. Specifically, it is possible to bound the dynamical critical exponent from below. We leave it for the future to use the RG circuit constructed above to determine its precise value.

Appendix A: Long range interactions in the classical model

Let us consider somewhat non-local classical hamiltonians. A motivation for attempting this is that the ground state of say a relativistic scalar field is positive definite and can be thought of as the square root of some statistical weight, but that weight will have power law decaying interactions if the field is massless.

Let $h = \sum_{ij} J_{ij} s_i s_j$ (with e.g. $J_{ij} \sim \frac{1}{|d(i,j)|^\alpha}$), so the classical partition sum is

$$\mathcal{Z} = \sum_s e^{-\beta h(s)} \propto \sum_s \int \prod_j dX_j e^{-\beta(\mathbf{i}\sum_i s_i X_i + \frac{1}{4}\sum_{ij} X_i J_{ij}^{-1} X_j)} \tag{A.1}$$

where J^{-1} is the matrix inverse of J.

The associated quantum state is:

$$|h\rangle = \frac{1}{\sqrt{\mathcal{Z}}} \sum_s e^{-\beta h(s)/2} |s\rangle \tag{A.2}$$

$$\propto \int [DX] e^{\frac{\beta}{4} X_i J_{ij}^{-1} X_j} \otimes_k (e^{-\mathbf{i}\beta X_k} |\uparrow\rangle_k + e^{\mathbf{i}\beta X_k} |\downarrow\rangle_k).$$

The introduction of the auxiliary field X gives a tensor product state:

$$\langle s|h\rangle \propto \int [DX] e^{-\frac{\beta}{4} X_i J_{ij}^{-1} X_j} e^{-\mathbf{i} s_k \beta X_k}, \tag{A.3}$$

i.e. it is a sum of product states where the local spin direction in each term is determined by the local auxiliary field. The auxiliary field acts like a local (imaginary) magnetic field.

Now any RG we know how to do on the X path integral tells us how to coarse-grain the state.

Quantum Laughlin plasma analogy

Another example which fits in this framework is the Laughlin wavefunction for incompressible abelian fractional quantum Hall states[39]. The statistical mechanics model for that case is the plasma of the "plasma analogy", *i.e.* a 2d classical gas of particles with logarithmic forces. This example seems different from the spin examples because the

wavefunction in question is in a state of definite particle number, in position space. Thinking of it this way gives a derivation of the associated Moore-Read CFT.

The norm of the Laughlin wavefunction at filling $\nu = 1/m$ is

$$\langle z_1..z_N | \text{laughlin}_m \rangle = \prod_{i<j} |z_i - z_j|^{2m} e^{-\sum_i |z_i|^2/2l^2} \equiv e^{-h(z)} \tag{A.4}$$

with $h(z) = \sum_{i=1}^{N} |z_i|^2/4l^2 - m \sum_{i<j} \log |z_{ij}|^2$. l is the magnetic length.

Usually one just thinks about the plasma analogy for the norm. But let's write the wavefunction itself using a lagrange multiplier to make the interaction in $h(z)$ local (in the z space):

$$|\text{laughlin}_m\rangle = \int d^N z \, |z_1..z_N\rangle \prod_{i<j} |z_{ij}|^m e^{-\sum_i |z_i|^2/4l^2}$$

$$= \int d^N z \, e^{-\sum_i |z_i|^2/2l^2} |z_1..z_N\rangle \tag{A.5}$$

$$\int [D\phi(z)] e^{-\int d^2 z \left(\frac{1}{4\pi} \partial_z \phi(z,\bar{z}) \bar{\partial}_z \phi(z,\bar{z}) + \phi(z,\bar{z}) \rho(z,\bar{z}) \right)}$$

where the source is $\rho(z,\bar{z}) = m \sum_{i=1}^{N} \delta^2(z - z_i)$. This is the $c = 1$ theory whose correlators give the wavefunction. that is:

$$\langle z_1..z_N | \text{laughlin}_m \rangle = \tag{A.6}$$

$$e^{-\sum_i |z_i|^2/2l^2} \int [D\phi(z)] e^{-\int d^2 z \left(\frac{1}{4\pi} \partial_z \phi(z,\bar{z}) \bar{\partial}_z \phi(z,\bar{z}) + \phi(z,\bar{z}) \rho(z,\bar{z}) \right)}$$

(We've suppressed some details above: a single copy the wavefunction itself is only the chiral piece of a free boson, whose path integral representation is a little problematic – it requires an extension of the configuration to an extra dimension and the use of the Chern-Simons action.)

Notice that in this case, the associated statistical mechanics model is an RG fixed point, despite the fact that the state in question is gapped – like known scale-invariant MERAs for non-chiral topologically-ordered gapped state.

Appendix B: Normalization of the Ising square root Hamiltonian and the limit $T \to 0$

The constants $c_i(\beta)$ in the normalization of the Hamiltonian (3.3) do not affect the statement that $|h\rangle$ is a ground-state. But they can be chosen to make the $\beta \to \infty$ zero-temperature limit more uniform. In particular, notice that

$$\begin{aligned} e^{-\frac{1}{2}\beta Z_1 Z_2} c_0(\beta) |\uparrow\downarrow\rangle &= c_0(\beta) e^{+\frac{1}{2}\beta} |\uparrow\downarrow\rangle, \\ e^{-\frac{1}{2}\beta Z_1 Z_2} c_0(\beta) |\uparrow\uparrow\rangle &= c_0(\beta) e^{-\frac{1}{2}\beta} |\uparrow\uparrow\rangle \end{aligned} \tag{B.1}$$

so if we choose $c_0(\beta) = e^{-\beta}$ the first expression stays finite as $\beta \to \infty$:

$$e^{-\frac{1}{2}\beta Z_1 Z_2} e^{-\beta} = e^{-\beta \mathbf{P}_0(Z_1 Z_2)} \tag{B.2}$$

where $\mathbf{P}_0(Z)$ is the projector onto $Z = 1$. Since $\mathbf{P}_0^2 = \mathbf{P}_0$, we have

$$e^{-\beta \mathbf{P}_0} = (1 - \mathbf{P}_0) + e^{-\beta} \mathbf{P}_0 = \mathbf{P}_1 + e^{-\beta} \mathbf{P}_0 \tag{B.3}$$

($\mathbf{P}_1(Z)$ projects onto $Z = -1$).

So we are led to take

$$c_i(\beta) = e^{-\frac{1}{2}\beta J n_i} \tag{B.4}$$

where n_i is the degree of the site i (i.e. the number of neighbors), and the hamiltonian can be written as:

$$\begin{aligned} \mathbf{H} &= \sum_i \left(-e^{-\frac{1}{2}n_i \beta J} X_i + \prod_{\langle i|j\rangle} e^{-\beta J \mathbf{P}_0(Z_i Z_j)} \right) \\ &= \sum_i \left(-e^{-\frac{1}{2}n_i \beta J} X_i + \prod_{\langle i|j\rangle} \left(\mathbf{P}_1(Z_i Z_j) + e^{-\beta} \mathbf{P}_0(Z_i Z_j) \right) \right) \end{aligned} \tag{B.5}$$

Notice that in the $\beta \to \infty$ limit, the paramagnetic term goes away. Further, the remaining term becomes just

$$\lim_{\beta \to \infty} \mathbf{H} = \sum_i \prod_{\langle i|j \rangle} \mathbf{P}_1(Z_i Z_j) . \tag{B.6}$$

This exacts a penalty for any disagreement between neighboring spins, and is zero on states where all the spins agree. This is consistent with the fact that the state $|h\rangle$ reduces to

$$\lim_{\beta \to +\infty} |h\rangle = \frac{1}{\sqrt{2}} \left(|\uparrow\uparrow\uparrow\uparrow \dots\rangle + |\downarrow\downarrow\downarrow\downarrow \dots\rangle \right) \tag{B.7}$$

in this limit.

Appendix C: Bounding the dynamical exponent of the critical 2d Ising square root state

Here is a variational bound on the dynamical critical exponent of the 2d Ising square-root quantum critical point. Briefly, it can be described as using the single-mode approximation as a variational state.

Consider the ansatz

$$|\phi\rangle = \sum_i Z_i |gs\rangle \equiv M |gs\rangle . \tag{C.1}$$

This state has the opposite eigenvalue of $\prod_i X_i$ from the groundstate. The energy expectation in this state provides an upper bound on the energy of the first excited state. This follows if we know that the first excited state is in the other symmetry sector. (Exact diagonalization on small systems indicates this to be true but a proof has not materialized.)

Its norm is

$$\langle \phi | \phi \rangle = Z \langle M^2 \rangle_{\text{ising}} \sim L^{4-\eta} Z \tag{C.2}$$

where the last relation holds at the critical point, and $\eta = 1/4$ is the twice the order parameter critical exponent.

So the lowest energy in the wrong-symmetry sector must be below

$$\frac{\langle \phi | H | \phi \rangle}{\langle \phi | \phi \rangle} \sim \frac{L^2}{L^{4-\eta} Z} E_i \tag{C.3}$$

where $E_i = \langle \phi | H_i | \phi \rangle$ is the expectation for a single term in H. The latter can be written as

$$E_i = \sum_s \langle \phi | s \rangle \sum_{s'} \langle s | H_i | s' \rangle \langle s' | \phi \rangle \tag{C.4}$$

Using $\langle \phi | s \rangle = M_s w_s^{1/2}$ where $w_s = e^{-\beta \sum_{\langle ij \rangle} s_i s_j}$ and $M_s = \sum_i s_i$, this is

$$E_i = \sum_s M_s w_s^{1/2} \left(e^{\beta s_i \sum_{\langle i|j \rangle} s_j} M_s w_s^{1/2} - M_{s'} w_{s'}^{1/2} \right) \tag{C.5}$$

where s and s' differ by flipping s_i, so that (as in the construction of H)

$$w_{s'}^{1/2} = w_s^{1/2} e^{\beta s_i \sum_{\langle i|j \rangle} s_j} . \tag{C.6}$$

So

$$E_i = \sum_s M_s w_s e^{\beta s_i \sum_{\langle i|j \rangle} s_j} (M_s - M_{s'}) \tag{C.7}$$

Now note that

$$w_s e^{\beta s_i \sum_{\langle i|j \rangle} s_j} = w_{s \backslash s_i} \tag{C.8}$$

where the RHS is the weight without the links containing the site i. Also:

$$M_s = \sum_{j \neq i} (s_j + s_i), \quad M_s - M_{s'} = 2s_i. \tag{C.9}$$

So

$$E_i = \sum_{\{s\} \setminus s_i} w_{s \setminus s_i} \sum_{s_i = \pm} \left(\sum_{j \neq i} s_j + s_i \right) 2s_i = 2Z(\backslash i) \tag{C.10}$$

where the RHS is the partition function of the ising model with the site i removed.

This quantity

$$Z(\backslash i) = Z \left\langle e^{\beta s_i \sum_{\langle i | j \rangle} s_j} \right\rangle \tag{C.11}$$

is bounded (on a lattice with coordination number 4) by

$$Ze^{-4\beta} < ZZ(\backslash i) < Ze^{+4\beta}. \tag{C.12}$$

This means that at large L it must be a positive constant times Z.

Therefore: the scaling of the excited state energy at the critical point is bounded above by

$$E_1 = \frac{c'}{L^z} > \frac{c}{L^{2-\eta}}, \tag{C.13}$$

and hence the dynamical exponent is bounded below by

$$z \geq 2 - \eta = 1.75. \tag{C.14}$$

Appendix D: Unitarity check

Unitary operators are in particular inner-product-preserving. Here we check explicitly that this property follows by construction for our unitaries made from the Levin-Nave RG tensors. Beginning from the ansatz (3.12) the goal is to check

$$\langle 000ijk | U_2^\dagger U_2 | i'j'k'000 \rangle \overset{?}{=} \delta_{i,i'} \delta_{j,j'} \delta_{k,k'}. \tag{D.1}$$

From the definition (3.12), we have

$$\langle ijk000 | U_2^\dagger = \sum_{ijkabc} \langle ijkabc | \sqrt{\frac{S_{abi} S_{bcj} S_{cak}}{T_{ijk}}} \tag{D.2}$$

(Note that we are using a convention where the arguments of the bra are in the same order as in the ket, and for simplicity we are assuming S, T are real.) Therefore the inner product

$$\langle ijk000 | i'j'k'000 \rangle = \delta_{i,i'} \delta_{j,j'} \delta_{k,k'}. \tag{D.3}$$

maps to

$$\langle ijk000 | U_2^\dagger U_2 | i'j'k'000 \rangle = \sum_{abc} \sum_{a'b'c'} \underbrace{\langle ijkabc | i'j'k'a'b'c' \rangle}_{= \delta_{aa'} \delta_{bb'} \delta_{cc'} \delta_{ii'} \delta_{jj'} \delta_{kk'}} \sqrt{\frac{S_{abi} S_{a'b'i'} S_{bcj} S_{b'c'j'} S_{cak} S_{c'a'k'}}{T_{ijk} T_{i'j'k'}}}$$

$$= \delta_{ii'} \delta_{jj'} \delta_{kk'} \sum_{abc} \frac{S_{abi} S_{bcj} S_{cak}}{T_{ijk}}$$

$$= \delta_{i,i'} \delta_{j,j'} \delta_{k,k'} = \langle ijk000 | i'j'k'000 \rangle. \tag{D.4}$$

For U_1 we have

$$\sum_e \langle abcde| \otimes \langle 0|_f \sqrt{T_{abe}T_{ecd}}U_1^\dagger = \sum_f \langle abcd0_e f| \sqrt{S_{acf}S_{fbd}} \tag{D.5}$$

So

$$\sum_{e,e'} \sqrt{T_{a'b'e'}T_{e'c'd'}T_{abe}T_{ecd}} \quad \cdot \quad \langle a'b'c'd'e'0_f| U_1^\dagger U_1 |abcde0_f\rangle$$

$$= \sum_{f,f'} \underbrace{\langle a'b'c'd'0_e f'|abcd0_e f\rangle}_{\delta^{a'b'c'd'f'}_{abcdf}} \sqrt{S_{a'c'f'}S_{f'b'd'}S_{acf}S_{fbd}}$$

$$= \delta^{a'b'c'd'}_{abcd} \underbrace{\sum_f S_{acf}S_{fbd}}_{=\sum_e T_{abe}T_{ecd}}$$

$$= \sum_{e,e'} \sqrt{T_{a'b'e'}T_{e'c'd'}T_{abe}T_{ecd}} \langle a'b'c'd'e'0_f|abcde0_f\rangle \tag{D.6}$$

[1] G. Vidal, "Class of Quantum Many-Body States That Can Be Efficiently Simulated," *Phys. Rev. Lett.* **101** (Sep, 2008) 110501, http://link.aps.org/doi/10.1103/PhysRevLett.101.110501.

[2] G. Evenbly and G. Vidal, "Class of Highly Entangled Many-Body States that can be Efficiently Simulated," *Phys. Rev. Lett.* **112** (Jun, 2014) 240502, http://link.aps.org/doi/10.1103/PhysRevLett.112.240502.

[3] B. Swingle and J. McGreevy, "Renormalization group constructions of topological quantum liquids and beyond," *ArXiv e-prints* (July, 2014) 1407.8203.

[4] G. Evenbly and G. Vidal, "Quantum Criticality with the Multi-scale Entanglement Renormalization Ansatz," *ArXiv e-prints* (Sept., 2011) 1109.5334.

[5] G. Evenbly and G. Vidal, "Entanglement renormalization in noninteracting fermionic systems," *Phys. Rev. B* **81** (Jun, 2010) 235102, http://link.aps.org/doi/10.1103/PhysRevB.81.235102.

[6] A. J. Ferris, "Fourier Transform for Fermionic Systems and the Spectral Tensor Network," *Phys. Rev. Lett.* **113** (Jul, 2014) 010401, 1310.7605, http://link.aps.org/doi/10.1103/PhysRevLett.113.010401.

[7] M. T. Fishman and S. R. White, "Compression of correlation matrices and an efficient method for forming matrix product states of fermionic Gaussian states," *Phys. Rev. B* **92** (Aug., 2015) 075132, 1504.07701.

[8] B. Swingle, "Entanglement Renormalization and Holography," *Phys.Rev.* **D86** (2012) 065007, 0905.1317.

[9] B. Swingle, "Constructing holographic spacetimes using entanglement renormalization," 1209.3304.

[10] T. Faulkner, M. Guica, T. Hartman, R. C. Myers, and M. Van Raamsdonk, "Gravitation from entanglement in holographic CFTs," *Journal of High Energy Physics* **3** (Mar., 2014) 51, 1312.7856.

[11] T. Hartman and J. Maldacena, "Time Evolution of Entanglement Entropy from Black Hole Interiors," *JHEP* **1305** (2013) 014, 1303.1080.

[12] B. Swingle and M. Van Raamsdonk, "Universality of Gravity from Entanglement," *ArXiv e-prints* (May, 2014) 1405.2933.

[13] J. C. Kimball, "The kinetic Ising model: Exact susceptibilities of two simple examples," *Journal of Statistical Physics* **21** (Sept., 1979) 289–300.

[14] I. Peschel and V. J. Emery, "Calculation of spin correlations in two-dimensional Ising systems from one-dimensional kinetic models," *Zeitschrift fur Physik B Condensed Matter* **43** (Sept., 1981) 241–249.

[15] D. S. Rokhsar and S. A. Kivelson, "Superconductivity and the Quantum Hard-Core Dimer Gas," *Phys.Rev.Lett.* **61** (1988) 2376–2379.

[16] R. Moessner, S. L. Sondhi, and P. Chandra, "Phase diagram of the hexagonal lattice quantum dimer model," *Phys. Rev. B* **64** (Sep, 2001) 144416, http://link.aps.org/doi/10.1103/PhysRevB.64.144416.

[17] R. Moessner, S. L. Sondhi, and E. Fradkin, "Short-ranged resonating valence bond physics, quantum dimer models, and Ising gauge theories," *Phys. Rev. B* **65** (Jan., 2002) 024504, cond-mat/0103396.

[18] E. Ardonne, P. Fendley, and E. Fradkin, "Topological order and conformal quantum critical points," *Annals Phys.* **310** (2004) 493–551, cond-mat/0311466.

[19] P. Horava, "Quantum Gravity at a Lifshitz Point," *Phys. Rev.* **D79** (2009) 084008, 0901.3775.

[20] C. Monthus, "Real-space renormalization for the finite temperature statics and dynamics of the Dyson Long-Ranged Ferromagnetic and Spin-Glass models," *ArXiv e-prints* (Jan., 2016) 1601.05643.

[21] F. Verstraete, M. M. Wolf, D. Perez-Garcia, and J. I. Cirac, "Criticality, the Area Law, and the Computational Power of Projected Entangled Pair States," *Physical Review Letters* **96** (June, 2006) 220601, quant-ph/0601075.

[22] M. Fannes, B. Nachtergaele, and R. F. Werner, "FINITELY CORRELATED STATES ON QUANTUM SPIN CHAINS," *Commun. Math. Phys.* **144** (1992) 443–490.

[23] F. Verstraete, V. Murg, and J. Cirac, "Matrix product states, projected entangled pair states, and variational renormalization group methods for quantum spin systems," *Advances in Physics* **57** (2008), no. 2 143–224, 0907.2796, http://dx.doi.org/10.1080/14789940801912366.

[24] U. Schollwöck, "The density-matrix renormalization group in the age of matrix product states," *Annals of Physics* **326** (Jan., 2011) 96–192, 1008.3477.

[25] R. Orus, "A Practical Introduction to Tensor Networks: Matrix Product States and Projected Entangled Pair States," *Annals Phys.* **349** (2014) 117–158, 1306.2164.

[26] M. Levin and C. P. Nave, "Tensor Renormalization Group Approach to Two-Dimensional Classical Lattice Models," *Phys. Rev. Lett.* **99** (Sep, 2007) 120601, http://link.aps.org/doi/10.1103/PhysRevLett.99.120601.

[27] Z. Y. Xie, H. C. Jiang, Q. N. Chen, Z. Y. Weng, and T. Xiang, "Second Renormalization of Tensor-Network States," *Phys. Rev. Lett.* **103** (Oct, 2009) 160601, http://link.aps.org/doi/10.1103/PhysRevLett.103.160601.

[28] Z. Y. Xie, J. Chen, M. P. Qin, J. W. Zhu, L. P. Yang, and T. Xiang, "Coarse-graining renormalization by higher-order singular value decomposition," *Phys. Rev. B* **86** (Jul, 2012) 045139, http://link.aps.org/doi/10.1103/PhysRevB.86.045139.

[29] A. García-Sáez and J. I. Latorre, "Renormalization group contraction of tensor networks in three dimensions," *Phys. Rev. B* **87** (Feb, 2013) 085130, http://link.aps.org/doi/10.1103/PhysRevB.87.085130.

[30] G. Evenbly and G. Vidal, "Tensor Network Renormalization," *Phys. Rev. Lett.* **115** (Oct, 2015) 180405, 1412.0732, http://link.aps.org/doi/10.1103/PhysRevLett.115.180405.

[31] G. Evenbly and G. Vidal, "Tensor network renormalization yields the multi-scale entanglement renormalization ansatz," *ArXiv e-prints* (Feb., 2015) 1502.05385.

[32] S. Yang, Z.-C. Gu, and X.-G. Wen, "Loop optimization for tensor network renormalization," *ArXiv e-prints* (Dec., 2015) 1512.04938.

[33] R. J. Creswick, H. A. Farach, and C. P. Poole, *Introduction to renormalization group methods in physics*. New York, USA: Wiley (1992) 409 p, 1992.

[34] B. Swingle, "Structure of entanglement in regulated Lorentz invariant field theories," *ArXiv e-prints* (Apr., 2013) 1304.6402.

[35] B. Czech, P. Hayden, N. Lashkari, and B. Swingle, "The Information Theoretic Interpretation of the Length of a Curve," *JHEP* **06** (2015) 157, 1410.1540.

[36] C. Holzhey, F. Larsen, and F. Wilczek, "Geometric and renormalized entropy in conformal field theory," *Nucl. Phys.* **B424** (1994) 443–467, hep-th/9403108.

[37] Z.-C. Gu, M. Levin, B. Swingle, and X.-G. Wen, "Tensor-product representations for string-net condensed states," *Phys. Rev. B* **79** (Feb., 2009) 085118, 0809.2821.

[38] M. Aguado and G. Vidal, "Entanglement Renormalization and Topological Order," *Physical Review Letters* **100** (Feb., 2008) 070404, 0712.0348.

[39] R. B. Laughlin, "Anomalous Quantum Hall Effect: An Incompressible Quantum Fluid with Fractionally Charged Excitations," *Phys. Rev. Lett.* **50** (May, 1983) 1395–1398.

[40] States of this form have a long history. The earliest references of which we are aware arise in the context of studies of kinetics of the Ising model[13,14], and more recent work includes[15–20].

[41] A construction of a PEPS representation of such states was made in[21]. In general a PEPS is not efficiently contractible however the technology we use to produce our circuits also permit these particular PEPS networks to be contracted. It would be quite interesting to understand if this is a more general connection - that a PEPS inherits contractibility from the existence of an RG circuit.

[42] Ordered groundstates of local Hamiltonians can have correlations which do not fall off with distance; such a system is gapless in the sense that the groundstate is degenerate in the thermodynamic limit. We will focus rather on examples where the correlations fall off with a nonzero power of the separation.

[43] Indeed, many improvements have been made upon the tensor renormalization group (TRG) procedure described in[26]. A few particularly successful innovations are: The addition of an extra step which takes into account the environment of the tensors, called SRG[27], is numerically dramatically more successful. It is not trivial to generalize the TRG to higher dimensions. Generalizations which accomplish this goal include HOSVD[28] and the work[29]. More recently, schemes were proposed[30,31] which are designed to remove additional types of correlations not addressed by TRG and to produce a better approximation to scale invariance. The latter work used a tensor network RG scheme on a 2d statistical model to produce a MERA for a 1d quantum model (the statistical model being interpreted as the Euclidean path integral of the quantum model); this is distinct from our work, e.g. the statistical model is *not* the Euclidean path integral of the quantum square root state model. It may, however, be usefully combined with our work, as we mention below. Even more recently, a possible further improvement has appeared[32].